Differential Antitumor Effects of IgG and IgM Monoclonal Antibodies and Their Synthetic Complementarity-Determining Regions Directed to New Targets of B16F10-Nex2 Melanoma Cells[1]

Andrey S. Dobroff*[,†], Elaine G. Rodrigues[†], Maria A. Juliano[‡], Dayson M. Friaça[§], Ernesto S. Nakayasu[¶], Igor C. Almeida[¶], Renato A. Mortara[†], Jacqueline F. Jacysyn[#], Gustavo P. Amarante-Mendes**, Walter Magliani[††], Stefania Conti[††], Luciano Polonelli[††] and Luiz R. Travassos[†]

*Department of Cancer Biology, The University of Texas MD Anderson Cancer Center, Houston, TX, USA; [†]Experimental Oncology Unit and Parasitology Division, Department of Microbiology, Immunology, Parasitology, Universidade Federal de São Paulo, São Paulo, Brazil; [‡]Department of Biophysics, Universidade Federal de São Paulo, São Paulo, Brazil; [§]Department of Pharmacology, Institute of Biomedical Sciences, Universidade de São Paulo, São Paulo, Brazil; [¶]Department of Biological Sciences, The Border Biomedical Research Center, University of Texas at El Paso, El Paso, TX, USA; [#]Department of Immunology, Institute of Biomedical Sciences, Universidade de São Paulo, Immunology Investigation Institute, National Institute of Science and Technology and Laboratory of Medical Investigation, Faculty of Medicine, Universidade de São Paulo, São Paulo, Brazil; **Department of Immunology, Institute of Biomedical Sciences, Universidade de São Paulo and National Institute of Science and Technology, São Paulo, Brazil; [††]Department of Pathology and Laboratory Medicine, Microbiology Section, Università degli Studi di Parma, Parma, Italy

Abstract

Malignant melanoma has increased incidence worldwide and causes most skin cancer–related deaths. A few cell surface antigens that can be targets of antitumor immunotherapy have been characterized in melanoma. This is an expanding field because of the ineffectiveness of conventional cancer therapy for the metastatic form of melanoma. In the present work, antimelanoma monoclonal antibodies (mAbs) were raised against B16F10 cells (subclone Nex4, grown in murine serum), with novel specificities and antitumor effects *in vitro* and *in vivo*. MAb A4 (IgG2ak) recognizes a surface antigen on B16F10-Nex2 cells identified as protocadherin β_{13}. It is cytotoxic *in vitro* and *in vivo* to B16F10-Nex2 cells as well as *in vitro* to human melanoma cell lines. MAb A4M (IgM) strongly reacted with nuclei of permeabilized murine tumor cells, recognizing histone 1. Although it is not cytotoxic *in vitro*, similarly with mAb A4, mAb A4M significantly reduced the number of lung nodules in mice challenged intravenously with B16F10-Nex2 cells. The V_H CDR3 peptide from mAb A4 and V_L CDR1 and CDR2 from mAb A4M showed significant cytotoxic activities *in vitro*, leading tumor cells to apoptosis. A cyclic peptide representing A4 CDR H3 competed with mAb A4 for binding to melanoma cells. MAb A4M CDRs L1 and L2 in addition to the antitumor effect also inhibited angiogenesis of human umbilical vein endothelial cells *in vitro*. As shown in the present work, mAbs A4 and A4M and selected CDR peptides are strong candidates to be developed as drugs for antitumor therapy for invasive melanoma.

Translational Oncology (2010) 3, 204–217

Introduction

Malignant melanoma is a deadly cancer of increasing incidence [1]. It is a heterogeneous solid tumor to which conventional therapy (e.g., chemotherapy and radiotherapy) is generally ineffective in its metastatic form [2]. New advances in the understanding of melanoma's microenvironment and the complexity of tumor development and immune response suggest that treatment of this disease may require a combination of procedures. Numerous studies have tested a variety of immunotherapeutic strategies in the treatment of advanced melanoma, including antitumor vaccines, interferon α, interleukin 2 (IL-2), dendritic cells, monoclonal antibodies (mAbs), and gene therapy [3–7].

The use of mAbs in cancer treatment has increased in the past few years. Originally, murine mAbs performed poorly in the clinic because of their short half-life and immunogenicity in the human host. Chimeric and humanized mAbs have overcome these disadvantages. MAbs are mostly active against membrane-bound target antigens. They can mediate signaling by cross-linking surface antigen that leads to cell death and may alter the cytokine milieu or enhance an active antitumor immune response [8–10]. They may block growth factor receptors, efficiently arresting proliferation of tumor cells [11]. Indirect effects include recruiting cells that exert antitumor antibody (Ab)-dependent cytotoxicity (ADCC), such as natural killer cells and macrophages [12]. MAbs can also bind complement, leading to complement-dependent cytotoxicity (CDC) [12,13]. The adverse effects associated with mAbs depend in part on the distribution of antigenic targets in normal tissues in addition to the intrinsic cytotoxicity of certain Abs. A further use of mAbs is to carry a toxin, cytotoxic agent, or radioisotope, specifically addressing it to the tumor's growing site [14,15]. MAbs can also act to modify the tumor microenvironment by inhibiting angiogenesis and by targeting integrins [16–18]. Several Abs are currently in preclinical and clinical trials to treat malignancies such as renal carcinoma, lymphomas, leukemia, breast, head and neck, ovarian, pancreatic, prostate, non–small cell lung, and colorectal cancers [19]. Molecular targets have been human epidermal growth factor receptors (HERs; epidermal growth factor receptor, [EGFR], and HER2), cMET receptor, insulin-like growth factor 1 receptor (IGF-1R), vascular endothelial growth factor (VEGF) and receptor (VEGFR) agents, and integrins $\alpha_5\beta_1$ and $\alpha_v\beta_3$. Aside from mAbs, a number of small-molecule inhibitors have also been tested in clinical and preclinical trials some already approved by the US Food and Drug Administration [20].

In melanoma, a restricted number of mAbs have been described with some success in tumor regression in clinical trials but with toxic adverse effects. *In vitro* studies have shown that mAb R24, a mouse immunoglobulin G (IgG) that recognizes the ganglioside GD3 [21], had specific antimelanoma properties. R24 binding to GD3 mediated ADCC as well as CDC, and infusion of R24 in patients with metastatic melanoma showed remarkable tumor regression in some of them [22]. Unfortunately, dose-dependent adverse effects restricted further use of mAb R24 [23]. To overcome the immunological tolerance to melanoma, a human anti-CTLA4 mAb, ipilimumab, is being tested as monotherapy and in combination with vaccines, IL-2, and dacarbazine. Overall response rates ranged from 13% to 22% in patients with stage IV metastatic disease [24]. Preclinical studies with a fully human Ab against melanoma cell adhesion molecule (MCAM/MUC18) have also shown promising results [25–27]. This Ab (ABX-MA1) had no effect on melanoma cell proliferation *in vitro*. However, it significantly inhibited tumor growth of metastatic mela-

noma cell lines injected subcutaneously in nude mice. ABX-MA1 treatment also suppressed lung metastasis of these melanoma cells [27]. MAbs represent, therefore, another modality to treat melanoma either alone or in combination with conventional chemotherapy or other antitumor agents.

Another approach in the immunotherapy of cancer patients involves peptides [28]. Peptides can be derived from tumor-associated antigens and be used to enhance the host immune response through interactions with and activation of T cells [29,30]. Further improvement of peptide vaccination, including the use of adjuvants, peptide-pulsed dendritic cells, multipeptide vaccination, addition of helper peptides, and peptide expression through the use of mini genes have made progress in the past few years [28,30–32]. Peptides can be synthesized with posttranslational modifications or protease-resistant peptide bonds to increase their stability *in vivo* [33]. Apart from immune peptides, there also are reports on the direct binding of peptides to tumor cells causing inhibition of tumor growth and killing cells by apoptosis. Antimicrobial peptides only in a few cases display antitumor activity [34]. Nevertheless, we showed that gomesin was cytotoxic to B16F10-Nex2 cells and human tumor cells *in vitro*. Topical treatment with gomesin of subcutaneously grafted melanoma in mice significantly reduced tumor growth [35].

Polonelli et al. [36] introduced the concept that short synthetic peptides corresponding to the sequences of immunoglobulin complementarity-determining regions (CDRs) may display antimicrobial, antiviral and antitumor activities regardless of the Ab specificity for a particular antigen. The high frequency of bioactive peptides based on CDRs suggests that Ig molecules could be sources of unlimited number of sequences potentially active against infectious agents and tumor cells.

Previously, we have shown that a murine mAb (A4) raised against B16F10 tumor cells was cytotoxic *in vitro* in a complement-mediated reaction and effectively thwarted tumor development in syngeneic mice [37]. A second antimelanoma mAb (A4M) was characterized, and in the present work, we describe their targets on tumor cells. Both mAbs significantly inhibited lung metastases, although only mAb A4 induced apoptosis of tumor cells *in vitro*. CDR peptides derived from both Abs also showed cytotoxicity against tumor cells. V_H CDR3–derived cyclic peptides from both mAbs showed characteristics of micro-Abs, including antitumor apoptotic activity in the case of mAb A4 H3.

Materials and Methods

Cell Lines and Reagents

The following cell lines were used in the present work: B16F10-Nex2, a subclone of B16F10 cell line originally obtained from the Ludwig Institute for Cancer Research, São Paulo branch; human melanoma cell lines (SKmel25, SKmel28, and Mel85); human umbilical vein endothelial cell line (HUVEC); human promyelocytic leukemia cell line (HL-60) and its transgenic mutants (Bcr-Abl, Bcl-2, and Bcl-X_L); hybridoma A4, raised against B16F10-Nex4 cells (*in vitro* cultured in murine serum-supplemented medium) as previously described [38]; and hybridoma A4M, isolated by subcloning A4 hybridoma. All cell lines and hybridomas were maintained in culture in RPMI 1640 medium pH 7.2, supplemented with 10% heat-inactivated fetal bovine serum, 10 mM HEPES (*N*-2-hydroxyethylpiperazine-*N*-2-ethanesulphonic acid), and 24 mM NaHCO$_3$, all from Gibco (Minneapolis, MN), and with 40 mg/L gentamicin sulfate (Hipolabor Farmacêutica, Belo

Horizonte, Brazil). Murine anti–pan-histone Abs were purchased from Boehringer Mannheim (Mannheim, Germany).

Monoclonal Antibodies and CDR-Based Synthetic Peptides

Hybridomas A4 and A4M were inoculated in pristane-inflamed peritoneum of nude female mice, and mAbs-containing ascites were collected. MAb A4 was purified as previously described [37], and mAb A4M was purified on Sephacryl S200 (Pharmacia LKB, Uppsala, Sweden) as described by Bouvet et al. [38]. Peptides based on CDR sequences of mAb A4 and mAb A4M were synthesized by the solid-phase and classic solution methods of peptide synthesis [39]. All the obtained peptides were purified by semipreparative HPLC on an Econosil C-18 column. The molecular mass and purity of synthesized peptides (≥94%) were checked by matrix-assisted laser desorption/ionization (MALDI)-time-of-flight (TOF) mass spectrometry, using TofSpec-E (Micromass, Manchester, UK). Irrelevant IgG 2a (17D) and IgM (1G6) mAbs, both raised against fungal (*Paracoccidioides*) antigens, were used as isotype controls.

Western Blot Analysis

B16F10-Nex2 total lysate (1×10^7 cells) was separated in 10% SDS–polyacrylamide gel electrophoresis and transferred to Immobilon P transfer membrane (Millipore, Billerica, MA). The membranes were washed in phosphate-buffered saline (PBS), pH 7.2, with Tween-20 (0.02%; PBS-T), and were blocked with 5% skimmed milk (Molico; Nestle, São Paulo, Brazil) in PBS-T overnight (ON) at 4°C. The blots were then probed ON at 4°C with mAb A4, A4M, or anti–pan-histone Abs. After 1 hour of incubation with anti-IgG or anti-IgM secondary Ab (1:2000) followed by 1 hour incubation with streptavidin-peroxidase, immunoreactive proteins were detected by chemiluminescent ELISA (CL-ELISA) according to the manufacturer's instructions (ECL detection system; Amersham Biosciences, Pittsburgh, PA). B16F10 nuclear extraction and histone detection by Western blot analysis were followed as previously described [35].

Immunoprecipitation

B16F10-Nex2 cells (1×10^8) were washed twice in PBS and lysed using lysis buffer (0.9% NaCl [Merck, Whitehouse Station, NJ], 0.01 M Tris-HCl [Gibco], pH 7.2, 0.01 M $MgCl_2$ [Merck], 0.2 M PMSF [Gibco], and 0.5% NP-40 [LKB-Produkter, Bromma, Sweden]). Total cell lysate (500 µg of protein) was incubated with 100 µg/ml of mAb A4 at 4°C ON on an orbital shaker. Protein A-Sepharose (Amersham Biosciences) was added (500 µl) to the sample and incubated at 4°C ON with shaking. Sample was collected by centrifugation at 3000 rpm for 5 minutes at 4°C and washed twice with PBS-T and once with PBS. Proteins were dissolved in SDS gel loading buffer and subjected to 10% SDS-PAGE.

Protein Identification by Liquid Chromatography–Tandem Mass Spectrometry

Immunoprecipitated sample was digested with trypsin as described by Stone and Williams [40]. Briefly, the samples were dissolved in 40 µl of 400 mM NH_4HCO_3 containing 8 M urea, and the disulfide bonds were reduced with 5 mM dithiothreitol for 15 minutes at 50°C. Cysteine residues were then alkylated with 10 mM iodoacetamide for 15 minutes at room temperature (RT). The reaction was diluted eight-fold, and 4 µg of trypsin (sequencing grade; Promega,

Madison, WI) was added and incubated ON at 37°C. The digestion was terminated with 1 µl of formic acid (FA), submitted to desalting using POROS R2 ziptips, as described elsewhere, and dried in a speed vac (Vacufuge; Eppendorf, Westbury, NY) [41].

Samples were redissolved in 20 µl of 0.1% FA, and 8 µl was loaded on a C18 trap column (0.25 µl; OptiPak, Oregon City, OR) coupled to a nano-HPLC system (1D-plus; Eksigent, Dublin, CA). After washing for 10 minutes with 2% acetonitrile (ACN)/0.1% FA in a flow rate of 5 µl/min, peptides were separated in a capillary reverse phase column (15 cm × 75 µm, 3-µm spheres; ProteoPep 2 [New Objective, Woburn, MA]). A gradient was set with 5% to 40% solvent B for 100 minutes (solvent A: 2% ACN/0.1% FA; solvent B: 80% ACN/0.1% FA) in a flow rate of 300 nl/min. Peptides eluted were analyzed online in a linear trap mass spectrometer (LTQ XL with ETD; Thermo Fisher Scientific, San Jose, CA). The 10 most abundant peaks were submitted to collision-induced dissociation (35% normalized collision energy) twice before being dynamically excluded for 2 minutes.

The MS/MS spectra of peptides from 600 to 4000 Da were converted to DTA using Bioworks (version 3.3.1; Thermo Fisher Scientific) with a threshold of 100 counts and 15 fragments. The spectra were searched against a database assembled with the mouse IPI (v3.25, downloaded on January 17, 2007, from http://www.ebi.ac.uk/IPI/IPImouse.html) and common contaminants (trypsin and keratin, downloaded on May 30, 2007, from http://www.ncbi.nlm.nih.gov/sites/entrez?db=Protein&itool=toolbar) sequences, using Sequest, (Thermo, Finnigan, San Jose, CA) [42]. All the sequences were set in the correct and inverse orientation forming, a database with a total of 104,850 sequences. The parameters of the database search were 2 Da for peptide mass tolerance, cysteine carbamidomethylation (fixed modification), methionine oxidation (variable modification), and a maximum of one missed cleaved site for trypsin digestion. The false-positive rate was calculated to be 1.2% to 2.9% depending on the data set after applying the following filters: DCn > 0.1; X_{corr} > 1.5, 2.2, 2.7 for singly, doubly, and triply charged peptides, respectively; distinct peptides; and a protein probability < 1e–3.

Confocal Microscopy

B16F10-Nex2 cells (2×10^3) were cultivated on round glass coverslips (13 mm) for 24 hours after fixation with 3.7% formaldehyde for 15 minutes at RT. Cells were then incubated with block solution (150 mM NaCl [Merck], 50 mM Tris [Invitrogen, Carlsbad, CA], 0.25% bovine serum albumin [BSA; Sigma, St Louis, MO], and 0.5% Tween-20 [Sigma], pH 7.2) for 1 hour at RT. A4M or anti–pan-histone Abs (5 mg/ml) were incubated for 12 hours at 4°C. After several washes in PBS, biotinylated antimouse IgM or antimouse IgG (1:500; Sigma) were incubated at RT for 1 hour after incubating with streptavidin–fluorescein isothiocyanate (FITC; 1:250; BD Biosciences, San Jose, CA). Alternatively, antimouse IgG rhodamine conjugate (1:250) was used to colocalize histones in the tumor cells. Staining of actin filaments and nuclei was performed with 0.3 µg/ml phalloidin-rhodamine conjugate (Invitrogen) and 50 µg/ml 4′6-diamidino-2-phenylindole, dihydrochloride (DAPI; Invitrogen), respectively, for 1 hour at RT. To remove histones from tumor cells, coverslips coated with B16F10 cells were previously treated with 0.4N sulfuric acid for 30 minutes on ice. After several washes in PBS, the reaction was carried out as described above. The coverslips were treated with a mounting medium (Vectashield; Vector Laboratories, Burlingame, CA) to reduce bleaching and were examined by laser scanning fluorescence confocal microscope (MRC 1024/UV System; Bio-Rad, Hercules, CA) equipped with a transmitted light detector for Nomarski differential interference contrast.

The images were obtained with a 40× 1.2 NA/water immersion PlanApo objective (Carl Zeiss MicroImaging, Inc, Thornwood, NY); Kalman averaging at least 20 frames using a 2-mm iris (pinhole).

In Vitro Cytotoxicity Analysis

MAbs or CDR peptides (linear or cyclic) were diluted in supplemented RPMI medium at different concentrations and incubated with 5×10^3 B16F10-Nex2 or human tumor cells in 96-well plates; cells were plated 24 hours before treatment. After ON incubation at 37°C, viable cells were counted in a Neubauer chamber (Electron Microscopy Sciences, Hatfield, PA) using Trypan blue. Alternatively, cell proliferation was measured using the Cell Proliferation Kit I (MTT; Boehringer Mannheim), an MTT-based colorimetric assay for quantification of cell proliferation and viability. Readings were made in an ELISA plate reader at 570 nm. Values are indicated as mean percentage variation of cell death and normalized to control. Each assay was performed in triplicate. Similar results were obtained in at least three independent experiments.

DNA Fragmentation Assay

B16F10-Nex2 cells as well as human melanoma cell lines were grown for 24 hours in 12-well plates (10^5 cells/well) and were then further incubated for 12 hours at 37°C with either the mAb A4 (100 μg/ml) or the synthetic CDR peptides (0.1 mM of A4 H3, 0.8 mM of A4M L1, and 0.6 mM of A4M L2). The DNA extraction and fragmentation analyses were carried out as previously described [36].

Apoptosis/Necrosis Detection

B16F10-Nex2 cells were grown for 24 hours in a six-well plate (5×10^5 cells/well) and further incubated with mAb A4 (100 μg/ml) for 6 and 12 hours at 37°C. For negative control, cells were incubated with irrelevant Ab at the same concentration. As positive control, cells were incubated with cisplatin at a final concentration of 400 μM per well. At the end, cells were harvested with cold PBS after three washes in the same buffer. Apoptotic/necrotic cells were detected using the ApoScreen Annexin V-FITC kit according to the manufacturer's instructions (Southern Biotechnology, Birmingham, AL). All experiments were conducted in triplicate. A representative picture is shown.

Cytofluorometric Analyses of Propidium Iodide Staining

The HL-60 cells were plated at 2×10^5/well in a six-well plate and incubated with CDR peptides at different concentrations for 12 hours or a fixed concentration (0.5 mM) and variable periods at 37°C. Cytofluorometric analyses of propidium iodide staining were performed according to Nicoletti et al. [43]. Briefly, both detached and attached cells were collected and incubated in a hypotonic fluorochrome solution (propidium iodide 50 μg/ml in 0.1% sodium citrate plus 0.1% Triton X-100). The propidium iodide fluorescence of each sample was analyzed by flow cytometry (BD, Franklin Lakes, NJ). Alternatively, HL-60 transgenic variants overexpressing antiapoptotic molecules such as Bcr-Abl, Bcl-2, and Bcl-X_L were treated with CDR peptides at 0.5 mM for 12 hours and analyzed as described above. Each sample was carried out in triplicates. Five individual experiments were analyzed.

In Vitro Angiogenesis Assay on Matrigel

The assay was prepared as previously described [44]. Briefly, BD Matrigel Matrix (BD Biosciences) was distributed in 96-well plates

and allowed to polymerize for 1 hour at 37°C. The HUVEC cells (5×10^3 cells/well) were suspended in 100 μl of RPMI medium supplemented with 0.2% of fetal calf serum in addition to the synthetic CDR peptides. The samples were added to each well and allowed to grow at 37°C for 18 hours. Images were captured at 8× magnification with a Sony (New York, NY) Cyber-shot camera coupled to a light inverted microscope. The number of proangiogenic structures (closed rings formed by intercellular projections) was counted from four different wells, and the average value was determined for each sample. As a control of the assay, HUVEC cells were plated on Matrigel without peptide addition.

Chemiluminescent-ELISA

CL-ELISA was carried out as previously described [37]. Briefly, B16F10-Nex2 cells (10^4 cells/well) were fixed with 0.5% glutaraldehyde for 12 hours at 4°C in a white opaque ELISA plate (Nunc, Roskilde, Denmark). After blocking with 1% BSA in PBS, 0.05% Tween 20 (BPT), purified mAbs A4 and A4M were incubated for 12 hours at 4°C. Biotinylated antimouse IgG or IgM (Sigma) and streptavidin-peroxidase (Sigma) were added at a dilution of 1:1000 in carbonate/bicarbonate buffer, pH 9.6, after incubating at 37°C for 30 minutes with gentle shaking. After several washes in BPT buffer, the reaction was detected by enhanced chemiluminescence using the ECL detection system following the manufacturer's instructions (GE
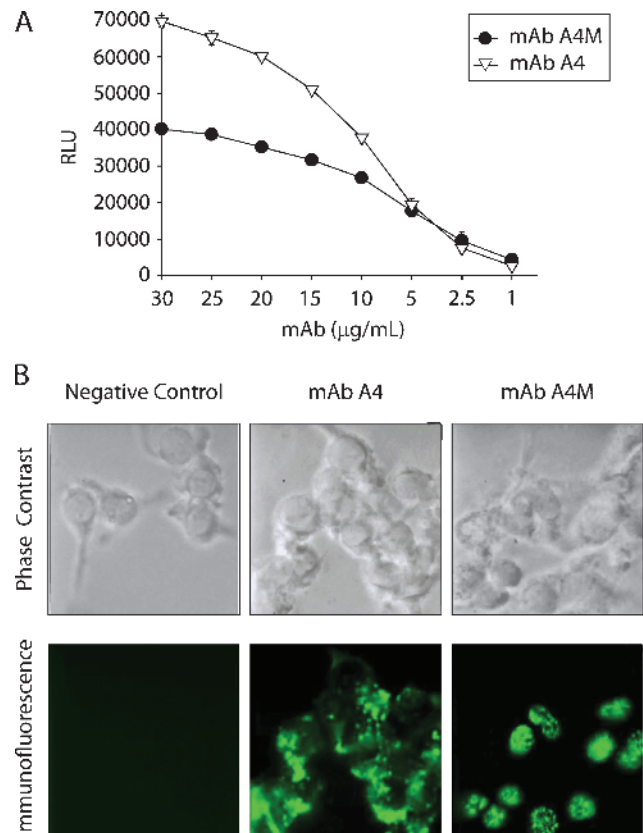

Figure 1. Reactivity of mAb A4 and mAb A4M with B16F10-Nex2 tumor cells. (A) mAb binding to melanoma cells evaluated in CL-ELISA. (B) Immunofluorescence of B16F10-Nex2 cells with mAb A4 and mAb A4M. Negative control, melanoma cells incubated with anti-Ig FITC alone.
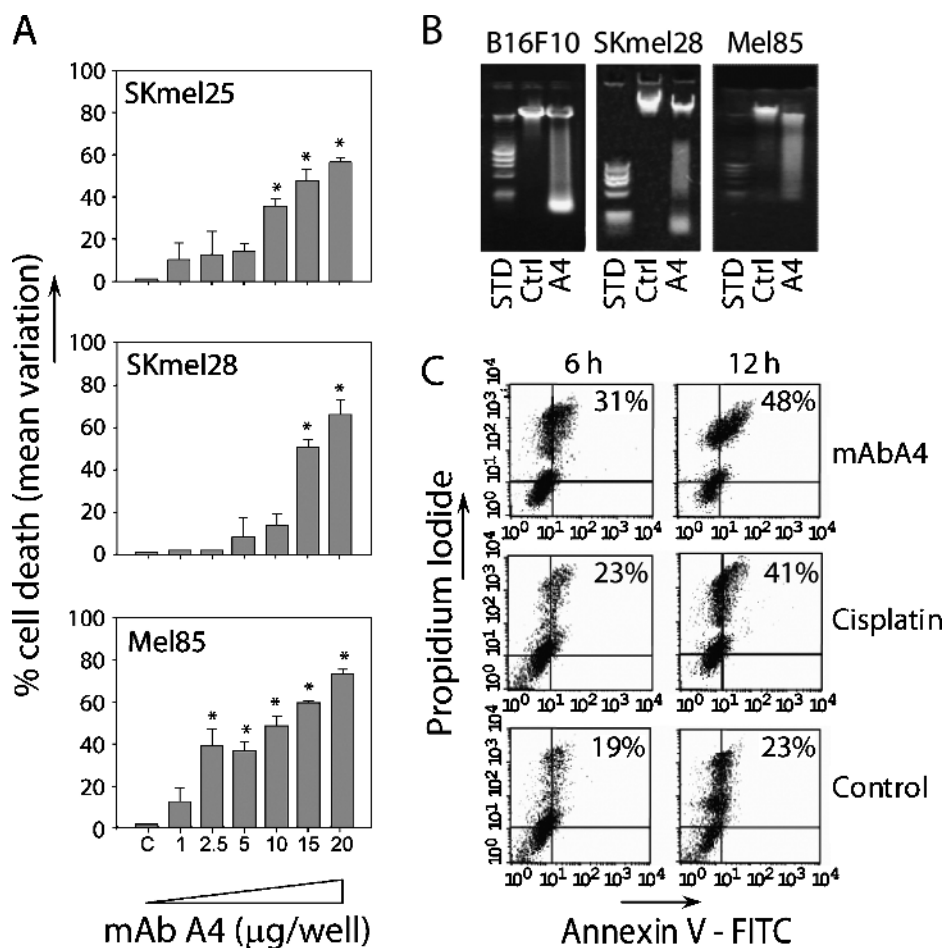
Figure 2. MAb A4 is cytotoxic in melanoma cell lines. (A) Inhibitory mAb A4 effect against human melanoma cell lines in the absence of complement. Cell viability was measured by MTT. Data are shown as mean percentage variation of cell death normalized to control. Control, cells incubated with an irrelevant antibody at 20 μg/well; *$P < .001$. (B) MAb A4 induced DNA degradation in B16F10-Nex2 and human melanoma cell lines. STD, 1 Kb Plus DNA Ladder; Ctrl, cells incubated with irrelevant antibody at the same concentration. (C) B16F10-Nex2 cells were treated with mAb A4, cisplatin, or an irrelevant antibody as described in Materials and Methods for 6 and 12 hours. Increased numbers of Annexin and propidium iodide (PI) double-positive cells were observed after mAb A4 and cisplatin incubation.

Healthcare Lifesciences, Piscataway, NJ). The chemiluminescence readings were obtained in a microplate luminometer (Cambridge Technology, Watertown, MA) and expressed as relative luminescent units. Alternatively, for the binding competition assay, synthetic CDR peptides were previously incubated at different concentrations with B16F10-Nex2–coated plates for 12 hours at 4°C. After several washes in BPT buffer, mAb A4 or A4M was added in triplicates at 10 μg/ml per well and further incubated for 12 hours at 4°C. The reaction was developed as described above.

Flow Cytometry (FACS)

B16F10-Nex2 cells (10^6/Eppendorf tube) were incubated with permeabilization buffer (PBS, pH 7.2, 0.5% saponin, 1% paraformaldehyde) for 20 minutes at 4°C. After several washes in PBS–saponin 0.5% (PBSs), CDR cyclic peptides (V_H cCDR3) derived from both mAb A4 and mAb A4M were added at three different concentrations (50, 10, and 1 μg per sample) for 1 hour at 4°C. After three washes in PBSs followed by blocking (1% BSA, PBSs), each sample was incubated with 10 μg/ml of the corresponding mAb for 1 hour at 4°C. Addition of the secondary Ab and data analysis were done as previ-

ously described. As negative control, cells were incubated only with the secondary Ab. For positive control, samples were treated with mAbs without peptide addition.

Animals, Tumor Growth, and Metastasis

Inbred male 8-week-old C57BL/6 mice were purchased from Centro de Desenvolvimento de Modelos Experimentais at the Federal University of São Paulo (UNIFESP). All animal experiments were approved by the Animal Experimental Ethics Committee of UNIFESP. Subcutaneous tumors were produced by injecting 5×10^4 B16F10-Nex2 cells (single-cell suspensions, >95% viability by Trypan blue exclusion test) in 0.1 ml of serum-free RPMI medium into the right flank of each mouse (five animals per group). Five days after challenge, the experimental group was treated intraperitoneally (i.p.) with mAb A4 (500 μg per mouse) and subsequent 100-μg doses after 7 days for 3 weeks. Tumor growth was recorded three times weekly with a caliper, and the survival of challenged animals was scored and statistically analyzed. The tumor volume was calculated using the formula: $V = 0.52 \times D_1^2 \times D_3$, where D_1 and D_3 are the short and long tumor diameters, respectively. Maximal volumes of 3 cm^3 were allowed

before killing. For experimental lung metastasis assay, 5×10^5 tumor cells, processed as described above, were injected into the tail veins of mice (0.1 ml per mouse). Five days after challenge, the experimental group was treated i.p. either with mAb A4 or with mAb A4M (500 µg per mouse) followed by a single i.p. administration of 100 µg of mAb A4 or A4M after 7 days. Twenty days later, animals were killed, their lungs were harvested, and the number of macroscopic surface tumor nodules was counted. Five mice were used in each group. Administration of an irrelevant Ab of same isotype was used as a negative control.

Statistical Analysis

Significant differences were assessed using Student's t test. All experiments were conducted two or more times. Reproducible results were obtained, and representative data are shown. The survival plots were analyzed by Kaplan-Meier log-rank test. In both tests, the differences were considered statistically significant when $P < .05$.

Results

MAb A4 and mAb A4M React with B16F10-Nex2 Cells

MAb A4 (IgG2ak) was obtained as previously described by immunization with whole B16F10-Nex4 cells grown in murine serum and mixed with Alum [37]. Subcloning of the hybridoma disclosed a second clone expressing mAb A4M (IgM). Both mAbs A4 and A4M strongly reacted with B16F10-Nex2 cells in a dose-dependent manner as shown by CL-ELISA (Figure 1*A*). Binding of mAb A4M was less intense than that of mAb A4.

Immunofluorescence assay showed that mAb A4M reacted mainly with nuclei of B16F10-Nex2 cells, whereas mAb A4 strongly reacted
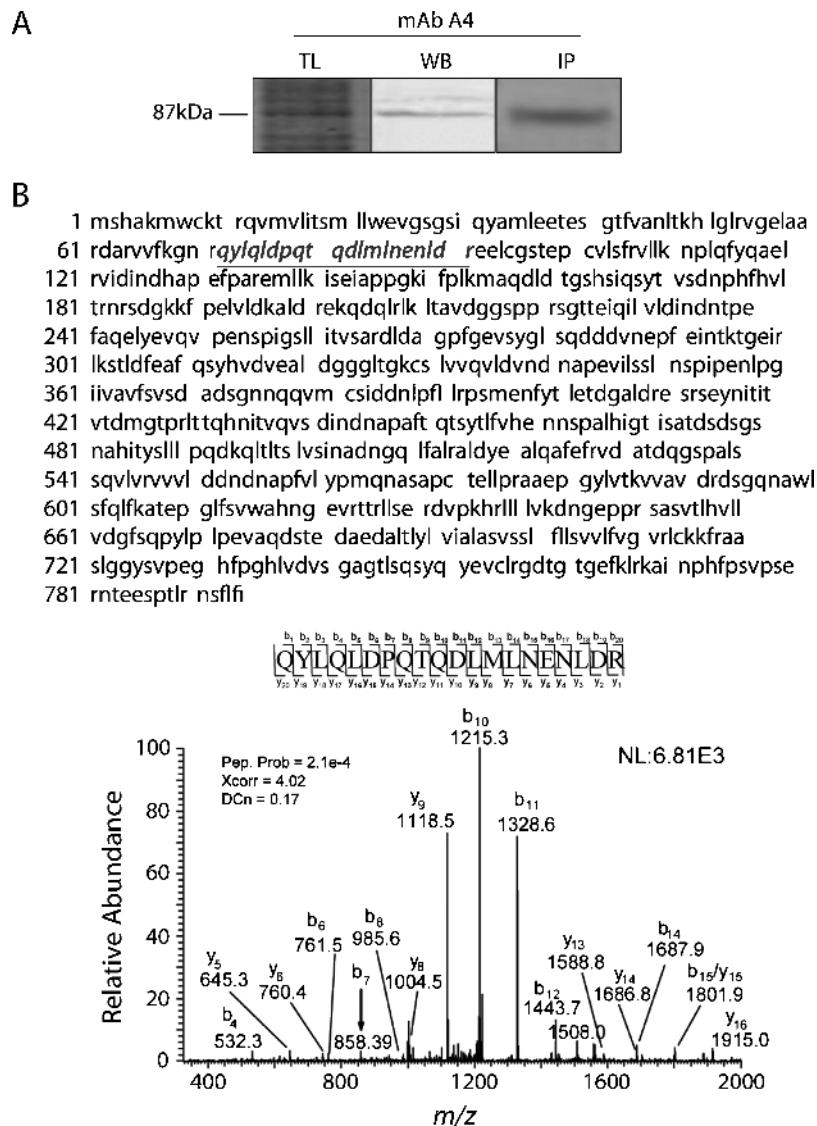

Figure 3. MAb A4 recognizes protocadherin β_{13} on melanoma cells. (A) TL of B16F10-Nex2 was examined for reactivity with mAb A4. TL, a band at 87 kDa was seen on SDS-PAGE; WB, a protein of identical molecular mass was recognized by mAb A4 in Western blot analysis; IP, the 87-kDa component was immunoprecipitated by mAb. (B) A mAb A4-immunoprecipitated sample was analyzed by LC–MS/MS, and the peptide shown underlined in bold italic and below was fully identified, being a characteristic of protocadherin β_{13} (complete sequence shown, 796 aa, calculated mol. wt. = 87,458).
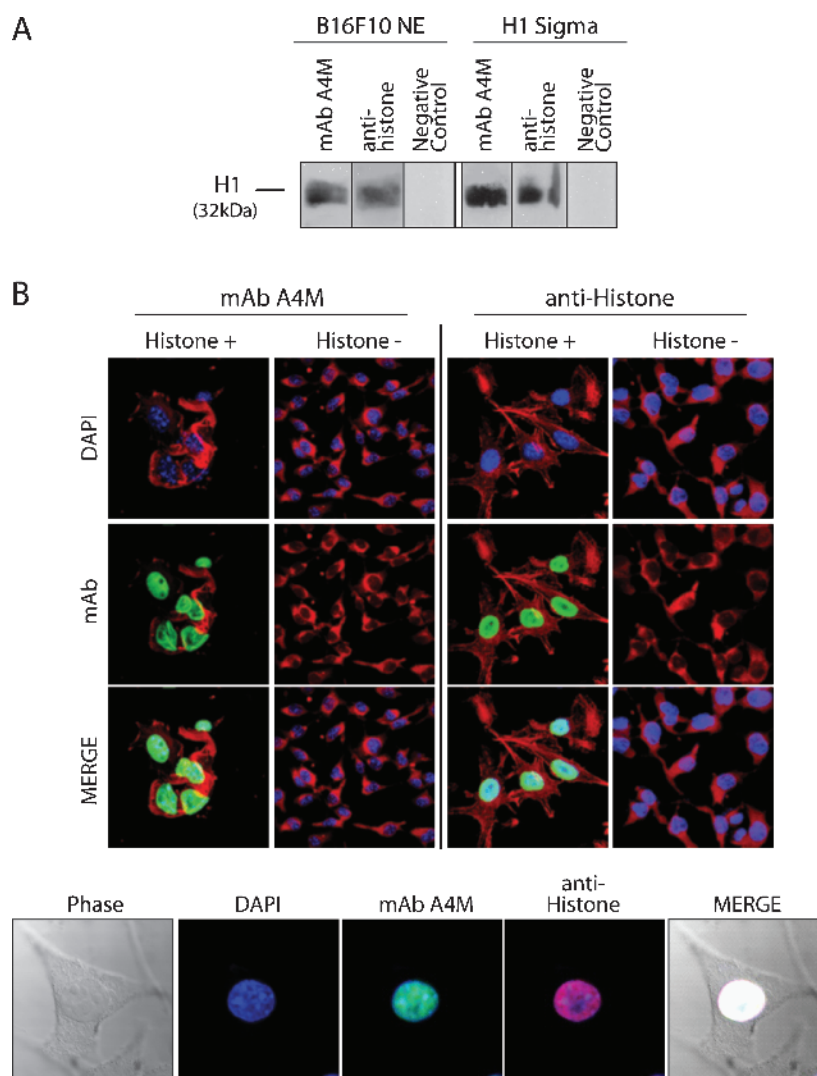
Figure 4. MAb A4M reacts with histone 1 in B16F10-Nex2 cells. (A) Western blot analysis of B16F10-Nex2 nuclear extract (NE) and H1 commercially purified calf thymus histone (Sigma) with mAb A4M and anti–pan-histone antibody. Negative control, with irrelevant mAb. (B) Confocal microscopy showing the mAb A4M reactivity on the nuclei of B16F10-Nex2 cells compared with antihistone antibody. Cells untreated (Histone +) and treated with sulfuric acid to remove histones (Histone −) are compared. Bottom panel: Colocalization of mAb A4M and antihistone reactions (MERGE). *Red* indicates phalloidin-rhodamine; *blue*, DAPI staining.

with components on the cell surface and cytoplasm of tumor cells (Figure 1*B*). As previously shown, mAb A4 recognizes a mimetope of melibiose. In contrast, binding of mAb A4M was not inhibited by any carbohydrate tested (data not shown). Also, both Abs bound to different peptides of a phage displayed a library of 9 to 12 aa peptides, showing that they indeed have different specificities (data not shown).

MAb A4 Induces Apoptosis in Melanoma Cell Lines through Binding to Protocadherin β13

We have shown that mAb A4 was cytotoxic to B16F10-Nex2 cells *in vitro*, independent of complement. Cytotoxic assays were also run without complement using three human melanoma cell lines (SKmel25, SKmel28, and Mel85). MAb A4 significantly reduced the cell viability of these cells by 50% at 15 μg/well compared with nontreated cells (Figure 2*A*).

Interestingly, mAb A4 treatment *in vitro* led to substantial morphological changes in tumor cells such as cell blebbing, shrinkage, and loss of adherence. B16F10-Nex2, SKmel28, and Mel85 cells

were then incubated with mAb A4, and DNA fragmentation was observed after 12 hours, suggesting the induction of apoptosis (Figure 2*B*). After treating with mAb A4 for 6 and 12 hours, adherent and detached B16F10-Nex2 cells were harvested and further analyzed by flow cytometry for Annexin V binding and propidium iodide incorporation. As depicted in Figure 2*C*, cells treated with mAb A4 for 12 hours had a twofold increase in double-positive cells compared with the negative control (48% and 23%, respectively). Such reactivity was similar to cisplatin treatment and showed that detached melanoma cells rapidly evolved from an apoptotic to necrotic stage incorporating propidium iodide.

To identify the mAb A4 ligand on melanoma cells, Western blot analysis was carried out using B16F10-Nex2 total lysate. MAb A4 recognized a protein of 87 kDa as seen in Figure 3*A* (*WB*). The immunoprecipitated sample with mAb A4 (Figure 3*A*, *IP*) was digested with trypsin and analyzed by liquid chromatography–tandem mass spectrometry (LC–MS/MS). After removing the hits from a sample immunoprecipitated by a control Ab and Ab sequences, we found only nine

candidates for the antigen recognized by mAb A4: cytochrome $P450$ 2A5 (IPI: IPI00123964.1), elongation factor 1-α_1 (IPI00307837.5), elongation factor 1-α_2 (IPI00119667.1), glycerol kinase-like protein 2 (IPI00123975.1), Golgi autoantigen (IPI00753818.1), L-lactate dehydrogenase B chain (IPI00229510.4), LOC544907 protein (IPI00462354.1), myeloid cysteine-rich protein (IPI00408687.1), and protocadherin β_{13} (IPI00129344.1; Figure 3B).

The latter was the only molecule that matched the antigen molecular mass of 87 kDa recognized by mAb A4. A very well characterized peptide, QYLQLDPQTQDLMLNENLDR, was found at 72 to 91 in the 796-aa protocadherin β_{13} glycoprotein. Murine and human surface-expressed protocadherin-β one-exon gene families show a high evolutionary conservation [45].

MAb A4M Recognizes Histone 1 in B16F10 Cells

MAb A4M strongly reacted with nuclei of B16F10-Nex2 cells, which is consistent with its lack of cytotoxicity to whole tumor cells *in vitro* with or without complement (not shown). Immunoblot analysis using B16F10-Nex2 nuclear extracts revealed that mAb A4M recognized a single protein band at 32 kDa corresponding to histone 1

(Figure 4A). To confirm mAb A4M specificity, we compared its reactivity with that of a commercial anti–histone 1 Ab. Both Abs reacted with purified calf thymus histone (H1; Sigma). Antihistone reactivities of both Abs were abolished after acid depletion of histones from B16F10-Nex2 nuclei (Figure 4B). Moreover, mAb A4M colocalized to the nucleus with antihistone Ab (Figure 4B, *lower panel*).

MAbs A4 and A4M Inhibit Tumor Growth and Metastases In Vivo

Mice challenged subcutaneously with B16F10-Nex2 cells were treated with mAb A4. As depicted in Figure 5A, treatment with mAb A4 rendered full protection against tumor growth (n = 5). All mAb-treated animals were alive 40 days after challenge compared with none in the untreated group ($P <$ .001; Figure 5B). MAb A4M was ineffective in the same conditions (not shown). We then evaluated the capacity of both A4 and A4M mAbs to inhibit metastases of melanoma cells. Mice were injected intravenously with B16F10-Nex2 cells and treated i.p. with mAbs A4 or A4M. A very significant reduction in the number of lung metastases was seen with both mAbs (mean values: A4 = 10, control = 150, P = .05; mAb A4M = 45, control = 155, $P <$ .05; Figure 5, C and D).
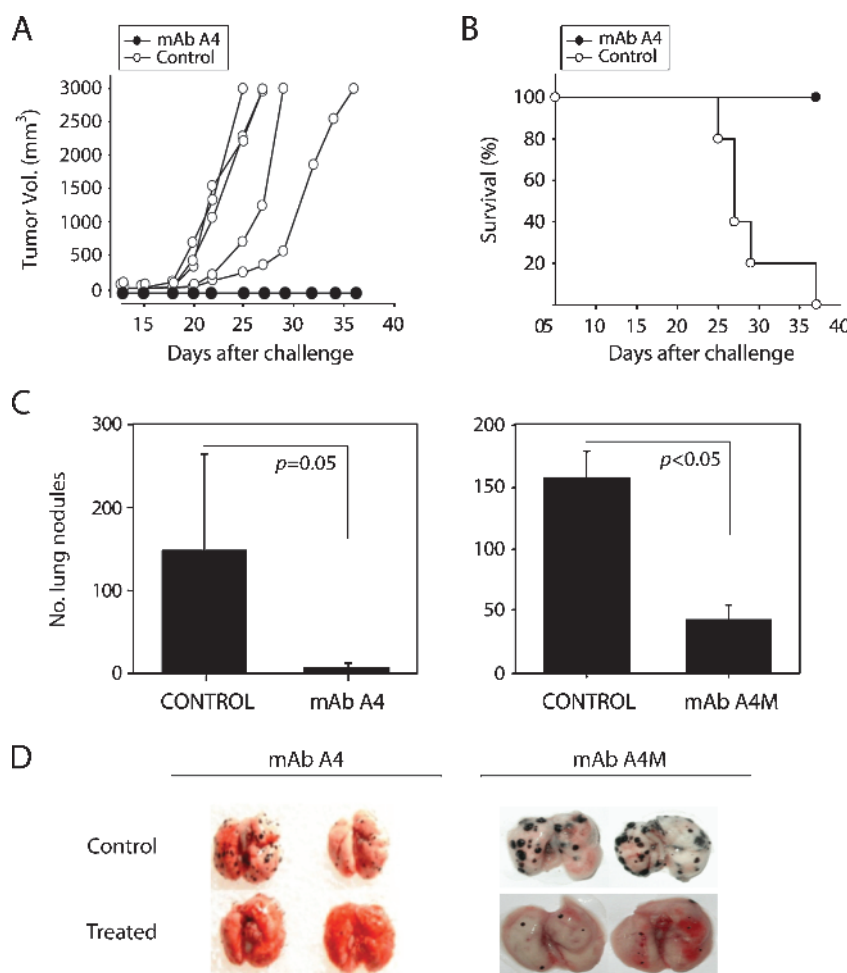

Figure 5. Antitumor effects of mAb A4 and mAb A4M. (A) MAb A4 injected i.p. led to inhibition of B16F10-Nex2 subcutaneous tumor growth (black circles, n = 5). Controls, animals injected i.p. with irrelevant antibody (white circles, n = 5). (B) Survival record of both groups treated with mAb A4 and the control group ($P <$ .001). (C) Effect of the mAb A4 and mAb A4M treatment on experimental lung metastases showing a significant decrease in their number with both mAbs (P = .05 and $P <$ .05, respectively). (D) Representative lungs from control and mAb-treated animals after 25 days of intravenous tumor challenge. Control, animals treated with irrelevant antibody at the same concentration.

Table 1. CDR Sequences of mAb A4 and mAb A4M.

CDR	mAb A4	mAb A4M
H1	DFAMS	EYTIH
H2	YISSAGSYIDYADTV	WFYPGSGSIKYNEKF
H3	IRDGHYGSTSHWYF	ARHEGRGWDYF
Cyclic H3	CIRDGHYGSTSHWYF*DVWG*C	CARHEGRGWDYF*DYWG*C
L1	TATSSVSSSYLH	RASGNIHNYLA
L2	STSNLAS	NVKTLA
L3	HQYHRSPP	QHFWSTPL

Italic: Cysteine added to obtain the cyclic peptide.
Underlined: Extended sequences as described by Morea et al. [48].

Synthetic Peptides On the Basis of the CDRs of mAb A4 and mAb A4M Induce DNA Degradation and Inhibit Cell Proliferation *In Vitro*

We have shown that synthetic CDR-related peptides derived from Abs with different specificities could display antimicrobial, antiviral, and antitumor effects *in vitro* and *in vivo* [36]. Presently, we examined the antitumor effects of CDRs from both mAbs A4 and A4M. Synthetic peptides corresponding to the CDRs 1 to 3 of V_L and 1 and 2 of V_H were tested in the linear form after Kabat's rules for their localization and size. CDR3 of V_H from both A4 and A4M were tested in the linear configuration and in a cyclic-extended form [46,47]. All sequences are shown in Table 1.

All CDRs from mAb A4 were screened *in vitro* against B16F10 cells. Interestingly, only mAb A4 CDR H3 was cytotoxic to B16F10 cells,
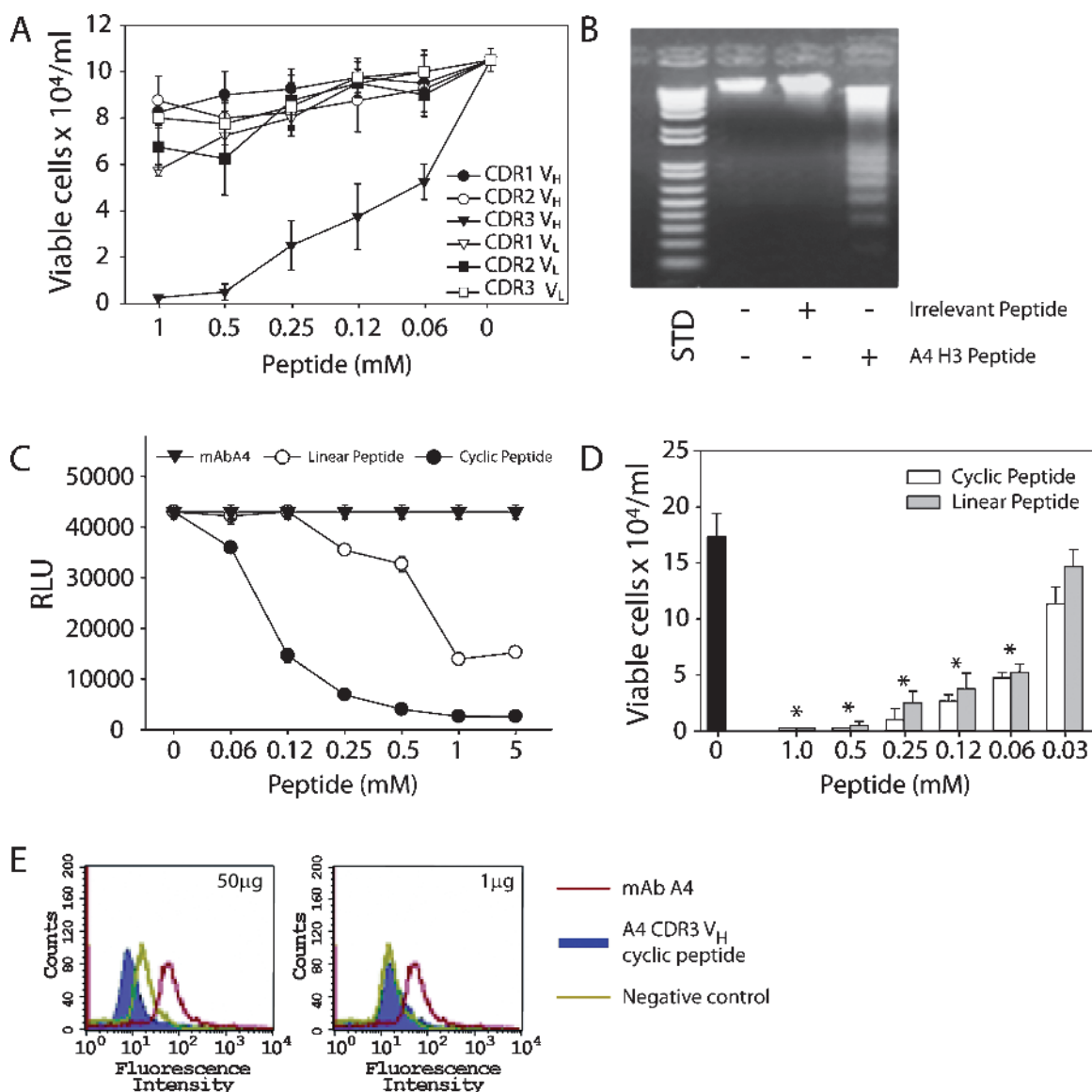

Figure 6. MAb A4 V_H CDR3 (H3) peptide is the only inhibitory CDR of mAb A4 (A). A4 H3 peptide induces DNA degradation in B16F10-Nex2 cells (B). STD, 1 Kb Plus DNA Ladder (Invitrogen). (C) Cyclic-extended and linear mAb A4 H3 peptides were tested for competition with mAb A4 in CL-ELISA. Peptides were incubated with tumor cells previously to addition of mAb A4 as described in Materials and Methods. (D) *In vitro* titration of cytotoxic effects of cyclic and linear mAb A4 H3 in B16F10-Nex2 cells. Black bar, untreated cells (*$P <$ .001). (E) Addition of cyclic-extended mAb A4 H3 peptide (50 μg) abrogates mAb A4 binding to B16F10-Nex2 cells (blue peak). Negative control, cells incubated with anti-IgG FITC alone. Positive control, mAb A4 alone (red peak).

Table 2. *In Vitro* Antitumor Activity of Synthetic mAb A4 CDR H3 and of mAb A4M CDRs L1 and L2 and Their Alanine-Substituted Derivatives (*asd*) against B16F10-Nex2 Melanoma Cells.

CDR	EC$_{50}$ (95% CI), M	
A4 H3	$6.00\ (4.117\text{-}7.883) \times 10^{-5}$	
A4M L1	$11.1\ (10.222\text{-}11.978) \times 10^{-4}$	
A4M L2	$26.1\ (22.304\text{-}29.896) \times 10^{-5}$	
mAb A4M L1 *asd*	EC$_{50}$ (95% CI), M	EC$_{50}$*asd*/EC$_{50}$L1
L1 R1A	$12.2\ (11.327\text{-}13.073) \times 10^{-4}$	1.09
L1 S3A	$12.2\ (10.041\text{-}14.359) \times 10^{-4}$	1.09
L1 G4A	$13.5\ (12.182\text{-}14.808) \times 10^{-4}$	1.21
L1 N5A	$10.8\ (9.923\text{-}11.677) \times 10^{-4}$	0.97
L1 I6A	$13.5\ (11.743\text{-}15.257) \times 10^{-4}$	1.21
L1 H7A	$11.5\ (10.622\text{-}12.378) \times 10^{-4}$	1.03
L1 N8A	$11.1\ (10.661\text{-}11.539) \times 10^{-4}$	1.00
L1 Y9A	$620\ (616.08\text{-}623.92) \times 10^{-4}$	55.85
L1 L10A	$621\ (619.57\text{-}620.43) \times 10^{-4}$	55.94
mAb A4M L2 *asd*	EC$_{50}$ (95% CI), M	EC$_{50}$*asd*/EC$_{50}$L2
L2 N1A	$1388.0\ (1378.0\text{-}1398.0) \times 10^{-5}$	53.38
L2 V2A	$41.6\ (40.166\text{-}43.034) \times 10^{-5}$	1.59
L2 K3A	$163.0\ (155.41\text{-}170.59) \times 10^{-5}$	6.25
L2 T4A	$2500.0\ (2482.1\text{-}2517.9) \times 10^{-5}$	95.78
L2 L5A	$49.0\ (37.525\text{-}60.475) \times 10^{-5}$	1.87

CI indicates confidence interval.

inhibiting 50% of tumor cell growth at 0.06 mM (Figure 6*A* and Table 2). Moreover, it led melanoma cells to apoptosis *in vitro*, inducing DNA degradation (Figure 6*B*). The possibility that A4 CDR H3 might act as a micro-Ab with several functional characteristics of the original mAb was initially tested in CL-ELISA. As seen in Figure 6*C*, the addition of the cyclic-extended form of A4 CDR H3 significantly inhibited the mAb A4 binding to melanoma cells. The linear A4 CDR H3 peptide was also inhibitory, but it was less active than the cyclic peptide. Both cyclic and linear A4 CDR H3 peptides were cytotoxic to B16F10-Nex2 cells, dramatically reducing the cell viability in a dose-dependent manner (Figure 6*D*). In addition, FACS analyses revealed that the cyclic A4 CDR H3 competed with mAb A4 for binding to the same antigen on B16F10-Nex2 cells, with 100% inhibition of mAb A4 binding at 50 μg of peptide (Figure 6*E*).

Likewise, CDR peptides derived from the mAb A4M were tested against B16F10-Nex2 cells *in vitro* (Figure 7*A*). Two CDR peptides, L1 and L2, were found to inhibit the tumor cell growth by 50% at 1.1 and 0.26 mM, respectively (Table 2). Alanine substitutions in the A4M CDR L1 peptide at the C-terminus (tyrosine and leucine residues) revealed that this region is essential for the cytotoxic activity. For the shorter A4M CDR L2 peptide, alanine substitutions of asparagine and mainly of threonine at positions 1 and 4 significantly reduced the cytotoxic activity of the CDR (Table 2).

Further experiments showed that A4M CDR L1 and L2 induced DNA degradation in B16F10-Nex2 cells (Figure 7*B*), suggesting that these peptides could also trigger apoptosis in tumor cells. Additional experiments using HL-60 leukemia cells and A4M CDR L2 revealed typical apoptotic alterations including surface blebs and nuclear fragmentation (data not shown). Furthermore, the DNA degradation was dose- and time-dependent (Figure 7*C*). When HL-60 cells overexpressing antiapoptotic molecules such as Bcr-Abl, Bcl-2, and Bcl-X$_{L}$ were used, the L2 peptide cytotoxicity (DNA degradation) was considerably inhibited (Figure 7*C*).

Because angiogenesis is another important therapeutic target for cancer treatment, we also tested A4M CDR peptides for the inhibi-

tion of endothelial cell (HUVEC) sprouting in Matrigel. The mAb A4M CDRs L1 and L2 and, less intensely, H1 and L3 significantly inhibited endothelial cell sprouting and intercellular connections in the 60% to 90% range ($P < .001$; Figure 7*D*).

Although cytotoxicity against B16F10-Nex2 cells was observed with L1 and L2 CDRs from mAb A4M, the Ab itself was not cytotoxic to whole tumor cells *in vitro*, indicating different mechanisms of action and binding properties of these agents. The A4M CDR H3 was not cytotoxic *per se* but was able to compete with mAb A4M for binding to melanoma cells. The cyclic form of A4M CDR H3 peptide inhibited mAb A4M binding to tumor cells as seen by FACS (Figure 7*E*) and by CL-ELISA where linear and cyclic forms of mAb A4M H3 inhibited Ab binding (Figure 7*F*). Thus, for mAbs A4 and A4M, H3 CDRs played roles of micro-Abs, representing an essential part of Ab-antigen recognition and, in some cases, displaying similar functional activities.

Discussion

Antibodies directed to tumor-associated differentiation antigens may have antitumor activities via CDC or ADCC as mediated by complement or immune effector cells, respectively, for example, natural killer and macrophages. These are not, however, the only mechanisms of Ab antitumor cytotoxicity. MAbs may have a direct antitumor activity without the participation of host components [48]. Abs do not cross the plasma membrane, unless it is permeabilized, but may be internalized by endocytosis. This may happen when the target is a receptor (e.g., receptors for transferrin, IL-2, EGF, TAPA-1 [the target of an antiproliferative antibody]) [49–52], but internalization of a mAb that recognized the Lewis Y carbohydrate epitope has also been reported [53,54]. This Ab (BR96) in the absence of complement or effector cells inhibited tumor cell DNA synthesis. However, it did not cause other alterations typical of apoptosis. In comparison, antimelanoma mAb A4 inhibited tumor cell growth *in vitro* in the absence of complement, recognized a surface receptor identified as protocadherin β_{13} (*Pcdh* β_{13}), and was seemingly internalized, causing DNA degradation not only in murine but also in human melanoma cells. Morphological changes caused by mAb A4 such as cell blebbing, shrinkage, and loss of adherence suggested the induction of apoptosis. Furthermore, mAb A4 exerted a strong protective effect *in vivo* against B16F10-Nex2 melanoma cells implanted subcutaneously or injected intravenously.

As Ab targets, protocadherins represent a large subgroup within the cadherin family of cell-cell adhesion molecules. Many of the protocadherins in mammals are expressed in the central nervous system with a role in tissue morphogenesis, synaptic transmission, and specific connections [55]. It is not surprising then that *Pcdh* β_{13} is expressed on melanoma cells that originally derived from the neural crest. *Pcdh* proteins may determine diverse neuronal connections that require tremendous diversity for either positive or negative (detoxification) effects. A tandem array of *Pcdh* variable exons, encoding distinct polypeptides, participates in generating such diversity [56,57]. Invasive tumor cells seem to have plasticity similar to multipotent embryonic progenitors [58]. Recent evidence revealed that when melanoma cells were transplanted in the neural crest of chick embryo, the microenvironment had the potential to control and reverse the metastatic phenotype. During migration along the neural crest pathways, mouse melanoma cells underwent apoptosis, which was assessed by anti–caspase 3 and TUNEL staining [59]. We hypothesize that *Pcdh* β_{13} might be a regulatory surface antigen of melanoma cells that, as shown in the present work, responded to mAb A4 binding leading cells to apoptosis. The binding
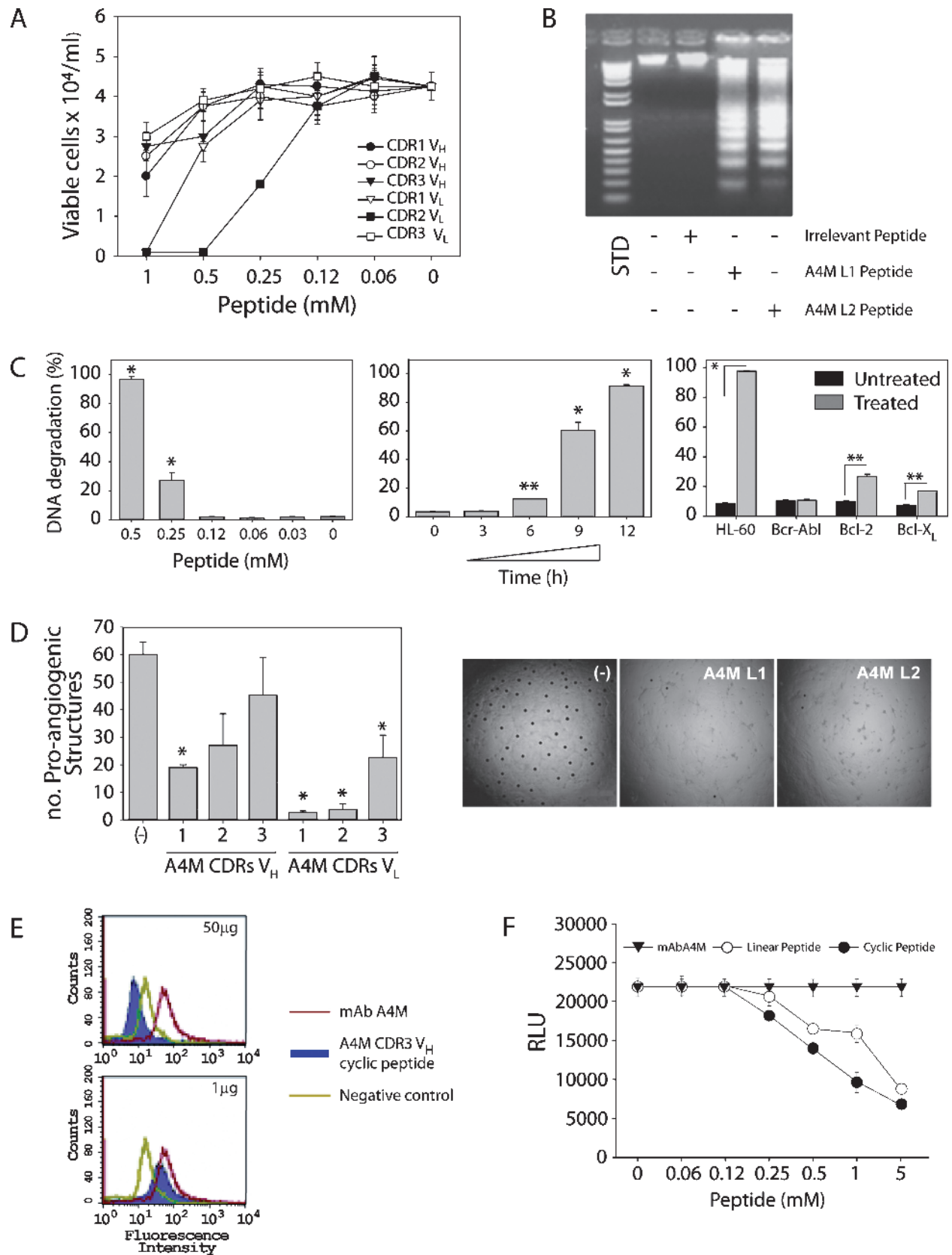
Figure 7. MAb A4M V_L CDR1 and 2 (L1, L2) are cytotoxic to B16F10-Nex2 melanoma cells (A) and induce DNA degradation in these cells (B). STD, 1 Kb Plus DNA Ladder. In human leukemia HL-60 cells, mAb A4M L2 peptide induces a dose- and time-dependent DNA degradation, which is blocked in HL-60 cells overexpressing antiapoptotic molecules (*$P < .001$, **$P < .01$) (C). Inhibition by mAb A4M CDRs L1 and L2 of HUVEC sprouting on Matrigel to form closed proangiogenic structures; *$P < .001$ relative to untreated control (−) (D). The mAb A4M cyclic-extended H3 inhibited mAb A4M binding to B16F10-Nex2 as shown by FACS (E) and by CL-ELISA (F). Negative control, cells incubated only with anti-IgM FITC. Positive control, mAb A4M alone (red).

motif in the protocadherin shows a mimicry to the disaccharide melibiose as determined before, but the nature of the epitope, either linear or conformational, is still unknown [37].

Whereas the obtainment of mAb A4 recognizing a minor component in B16F10-Nex2 melanoma might be attributed to the immunization of mice with tumor cells grown in mouse serum–supplemented medium, thus avoiding xenogeneic contamination, mAb A4M seemed to respond as an autoimmune IgM reacting with nuclear histone H1. Antihistone Abs have been detected in the sera of patients with various autoimmune diseases and are predominantly directed to histone H1. The preferential reactivity of mAb A4M with a nuclear component was clearly shown in permeabilized tumor cells. Acid extraction of histones abolished the reactivity of the Ab. Moreover, mAb A4M did not react with DNA as tested in a *Crithidia*-DNA binding test (not shown). In contrast to mAb A4, A4M was not cytotoxic *in vitro*. If, however, the tumor cells had previously been permeabilized by a membrane-interacting peptide (e.g., the antimicrobial gomesin), mAb A4M showed additive cytotoxic activity [35].

MAb A4M also bound to intact melanoma cells *in vitro* with less affinity compared with mAb A4. By examining a biotinylated surface proteoma of B16F10-Nex2 melanoma cells kept for 24 hours in a fetal calf serum–free medium, evidence was obtained for the presence of histone H2B and histone H1.2 (unpublished data). It cannot be ruled out, however, that mAb A4M surface reactivity might also involve a conformational antigen mimicry. It has been reported that a mAb to Lewis Y/Lewis b carbohydrate epitopes also bound to bovine histone H1 and human histone H1.2 in a concentration-dependent manner [60]. Histone H2B was also recognized by the lung cancer–specific human mAb HB4C5 [61]. Furthermore, anti-DNA auto-Abs were found to cross-react with cell surface proteins from different cell types [62]. Then, it seems that autoimmune antinuclear Abs have a potential to cross-react with many other antigens of completely different structures.

Surprisingly, mAb A4M was protective *in vivo* against lung colonization by melanoma cells similarly to mAb A4. Antitumor activity was not mediated by complement, as it was the case with several polyclonal IgM Abs with antitumor activity [63,64]. There is evidence showing that some IgM molecules recognizing cell surface carbohydrates may have a tumor-suppressive activity by a macrophage-dependent mechanism [65]. Yet, another protective mechanism could involve an inflammatory response enhanced by IgM reactivity with necrotic tumor cells. IgM Abs that recognize internal antigens in necrotic metastatic melanoma cells can also be used as carriers of radioactive isotopes as shown with antimelanin Abs, thus becoming a valuable tool for radioimmunotherapy [66,67]. Therefore, both mAbs A4 and A4M of the present work represent promising tools for the immunotherapy for metastatic melanoma as shown in preclinical evaluation studies.

Polonelli et al. [36] obtained experimental evidence supporting the concept that peptides derived from internal sequences of immunoglobulins could display, with high frequency, antimicrobial, antiviral, and antitumor activities *in vitro*, *ex vivo*, and *in vivo*. This was based on a series of previous contributions, recently reviewed by Magliani et al. [72], which showed that Ig fragments, tested as synthetic peptides derived from CDR domains and/or framework regions of immunoglobulins, had broad antibiotic properties similar to precursors and actual protective molecules of native immunity [68–73]. The bioactivity of these peptides was generally independent of Ab specificity, although it is well known that V_H CDR3 (H3) may, in several instances, reproduce Ab-specific binding to the antigen and display the same biological activity [74–76]. The peptide (H3) with such properties is

called a micro-Ab [47,77]. Presently, we extended these studies to mAbs A4 and A4M, with the perspective of additional antitumor molecules being unraveled.

Both mAbs A4 and A4M generated micro-Abs represented by peptide sequences of V_H CDR3 tested as linear peptides or as extended H3 sequences made cyclic by adding Cys at the C-terminal and forming a Cys-Cys bond under oxidation conditions [46]. Linear and cyclic H3 peptides competed with mAbs A4 and A4M for binding to B16F10-Nex2 cells. The cyclic H3 form of mAb A4 showed greater affinity for melanoma cells than the linear H3 form. Both linear and cyclic mAb A4 H3 peptides inhibited growth of tumor cells, and the linear form caused DNA degradation, suggesting that the H3 peptide as well as the mAb A4 induced apoptosis in B16F10-Nex2 cells.

The only CDR from mAb A4 with antitumor activity was V_H CDR3. In contrast, V_H CDR3 from mAb A4M was not cytotoxic, thus acting as mAb A4M *in vitro*. Conversely, V_L CDR 1 and V_L CDR 2 from mAb A4M inhibited growth of B16F10-Nex2 cells *in vitro* and caused DNA degradation in the tumor cells. CDR L2, studied in greater detail, was shown to degrade DNA in a dose- and time-dependent manner, and its apoptotic effect was inhibited by the antiapoptotic Bcr-Abl, Bcl-2, and Bcl-X$_L$ molecules transfected in HL-60 cells [78]. The antitumor effect of mAb A4M CDR L1 was significantly inhibited by replacing the last two hydrophobic residues at the C-terminal by alanine, thus suggesting a hydrophobic interaction with the tumor cell membrane. The shorter mAb A4M CDR L2 sequence lost its antitumor effect *in vitro* by alanine replacement of asparagine and lysine but mainly of threonine on the fourth position, suggesting a specific interaction with a surface receptor on the tumor cell. Remarkably, both mAb A4M CDRs L1 and L2 inhibited angiogenesis of HUVEC, which could also suggest that these peptides may be protective *in vivo* similarly as peptide C7 H2 and HuA L1 studied before [36].

In the present work, therefore, we describe two new specificities for antimelanoma mAbs showing that both mAbs A4 (IgG2a) and A4M (IgM) are protective *in vivo* against invasive B16F10-Nex2 cells in a model of lung metastasis. MAb A4 but not mAb A4M was cytotoxic *in vitro* and protective in the subcutaneous model of tumor development. An apoptotic micro-Ab was recognized in the V_H CDR3 of mAb A4, and two V_L CDRs (L1 and L2) of mAb A4M induced apoptosis of melanoma cells and inhibited angiogenesis. They not only supported the concept of intrinsic bioactivity of Ig peptide sequences but also emerged as promising agents for antitumor therapy along with the tumor-suppressive mAbs.

Acknowledgments

References
[1] Jemal A, Siegel R, Ward E, Hao Y, Xu J, Murray T, and Thun MJ (2008). Cancer statistics, 2008. *CA Cancer J Clin* **58**, 71–96.
[2] Terheyden P, Tilgen W, and Hauschild A (2008). Recent aspects of medical care of malignant melanoma. *J Dtsch Dermatol Ges* **6**, 868–878.
[3] Komenaka I, Hoerig H, and Kaufman HL (2004). Immunotherapy for melanoma. *Clin Dermatol* **22**, 251–265.

[4] Vulink A, Radford KJ, Melief C, and Hart DN (2008). Dendritic cells in cancer immunotherapy. *Adv Cancer Res* **99**, 363–407.

[5] Eggermont AM and Schadendorf D (2009). Melanoma and immunotherapy. *Hematol Oncol Clin North Am* **23**, 547–564.

[6] Atkins MB (1998). Immunotherapy and experimental approaches for metastatic melanoma. *Hematol Oncol Clin North Am* **12**, 877–902.

[7] Sarkar D, Su ZZ, Park ES, Vozhilla N, Dent P, Curiel DT, and Fisher PB (2008). A cancer terminator virus eradicates both primary and distant human melanomas. *Cancer Gene Ther* **15**, 293–302.

[8] Stanglmaier M, Reis S, and Hallek M (2004). Rituximab and alemtuzumab induce a nonclassic, caspase-independent apoptotic pathway in B-lymphoid cell lines and in chronic lymphocytic leukemia cells. *Ann Hematol* **83**, 634–645.

[9] Weiner GJ (2007). Monoclonal antibody mechanisms of action in cancer. *Immunol Res* **39**, 271–278.

[10] Kunpeng Z, Yugang W, Jugao C, Yan L, Beifen S, and Yuanfang M (2009). The construction and expression of a novel chimeric anti-DR5 antibody. *Hybridoma (Larchmt)* **28**, 101–105.

[11] Gridelli C, Maione P, Ferrara ML, and Rossi A (2009). Cetuximab and other anti–epidermal growth factor receptor monoclonal antibodies in the treatment of non–small cell lung cancer. *Oncologist* **14**, 601–611.

[12] Nakano K, Orita T, Nezu J, Yoshino T, Ohizumi I, Sugimoto M, Furugaki K, Kinoshita Y, Ishiguro T, Hamakubo T, et al. (2009). Anti–glypican 3 antibodies cause ADCC against human hepatocellular carcinoma cells. *Biochem Biophys Res Commun* **378**, 279–284.

[13] Ragupathi G, Liu NX, Musselli C, Powell S, Lloyd K, and Livingston PO (2005). Antibodies against tumor cell glycolipids and proteins, but not mucins, mediate complement-dependent cytotoxicity. *J Immunol* **174**, 5706–5712.

[14] McCarron PA, Olwill SA, Marouf WM, Buick RJ, Walker B, and Scott CJ (2005). Antibody conjugates and therapeutic strategies. *Mol Interv* **5**, 368–380.

[15] Fleckenstein G, Osmers R, and Puchta J (1998). Monoclonal antibodies in solid tumours: approaches to therapy with emphasis on gynaecological cancer. *Med Oncol* **15**, 212–221.

[16] Colman RW (2002). Inhibition of angiogenesis by a monoclonal antibody to kininogen as well as by kininostatin which block proangiogenic high molecular weight kininogen. *Int Immunopharmacol* **2**, 1887–1894.

[17] Yan X, Lin Y, Yang D, Shen Y, Yuan M, Zhang Z, Li P, Xia H, Li L, Luo D, et al. (2003). A novel anti-CD146 monoclonal antibody, AA98, inhibits angiogenesis and tumor growth. *Blood* **102**, 184–191.

[18] Song JS, Sainz IM, Cosenza SC, Isordia-Salas I, Bior A, Bradford HN, Guo YL, Pixley RA, Reddy EP, and Colman RW (2004). Inhibition of tumor angiogenesis *in vivo* by a monoclonal antibody targeted to domain 5 of high molecular weight kininogen. *Blood* **104**, 2065–2072.

[19] Dalle S, Thieblemont C, Thomas L, and Dumontet C (2008). Monoclonal antibodies in clinical oncology. *Anticancer Agents Med Chem* **8**, 523–532.

[20] Ma WW and Adjei AA (2009). Novel agents on the horizon for cancer therapy. *CA Cancer J Clin* **59**, 111–137.

[21] Pukel CS, Lloyd KO, Travassos LR, Dippold WG, Oettgen HF, and Old LJ (1982). GD3, a prominent ganglioside of human melanoma. Detection and characterisation by mouse monoclonal antibody. *J Exp Med* **155**, 1133–1147.

[22] Houghton AN, Mintzer D, Cordon-Cardo C, Welt S, Fliegel B, Vadhan S, Carswell E, Melamed MR, Oettgen HF, and Old LJ (1985). Mouse monoclonal IgG3 antibody detecting GD3 ganglioside: a phase I trial in patients with malignant melanoma. *Proc Natl Acad Sci USA* **82**, 1242–1246.

[23] Soiffer RJ, Chapman PB, Murray C, Williams L, Unger P, Collins H, Houghton AN, and Ritz J (1997). Administration of R24 monoclonal antibody and low-dose interleukin 2 for malignant melanoma. *Clin Cancer Res* **3**, 17–24.

[24] Weber J (2008). Overcoming immunologic tolerance to melanoma: targeting CTLA-4 with ipilimumab (MDX-010). *Oncologist* **13**(suppl 4), 16–25.

[25] Zigler M, Villares GJ, Lev DC, Melnikova VO, and Bar-Eli M (2008). Tumor immunotherapy in melanoma: strategies for overcoming mechanisms of resistance and escape. *Am J Clin Dermatol* **9**, 307–311.

[26] Melnikova VO and Bar-Eli M (2006). Bioimmunotherapy for melanoma using fully human antibodies targeting MCAM/MUC18 and IL-8. *Pigment Cell Res* **19**, 395–405.

[27] Mills L, Tellez C, Huang S, Baker C, McCarty M, Green L, Gudas JM, Feng X, and Bar-Eli M (2002). Fully human antibodies to MCAM/MUC18 inhibit tumor growth and metastasis of human melanoma. *Cancer Res* **62**, 5106–5114.

[28] Shadidi M and Sioud M (2003). Selective targeting of cancer cells using synthetic peptides. *Drug Resist Updat* **6**, 363–371.

[29] Apostolopoulos V (2009). Peptide-based vaccines for cancer: are we choosing the right peptides? *Expert Rev Vaccines* **8**, 259–260.

[30] Brinkman JA, Fausch SC, Weber JS, and Kast WM (2004). Peptide-based vaccines for cancer immunotherapy. *Expert Opin Biol Ther* **4**, 181–198.

[31] Miao Y and Quinn TP (2008). Peptide-targeted radionuclide therapy for melanoma. *Crit Rev Oncol Hematol* **67**, 213–228.

[32] Miao Y, Hylarides M, Fisher DR, Shelton T, Moore H, Wester DW, Fritzberg AR, Winkelmann CT, Hoffman T, and Quinn TP (2005). Melanoma therapy via peptide-targeted {alpha}-radiation. *Clin Cancer Res* **11**, 5616–5621.

[33] Purcell AW, McCluskey J, and Rossjohn J (2007). More than one reason to rethink the use of peptides in vaccine design. *Nat Rev Drug Discov* **6**, 404–414.

[34] Daffre S, Bulet P, Spisni A, Ehret-Sabatier L, Rodrigues EG, and Travassos LR (2008). Bioactive natural peptides. In *Studies in Natural Products Chemistry*. A-u- Rahman (Ed). Elsevier, Oxford, UK. pp. 597–691.

[35] Rodrigues EG, Dobroff AS, Cavarsan CF, Paschoalin T, Nimrichter L, Mortara RA, Santos EL, Fazio MA, Miranda A, Daffre S, et al. (2008). Effective topical treatment of subcutaneous murine B16F10-Nex2 melanoma by the antimicrobial peptide gomesin. *Neoplasia* **10**, 61–68.

[36] Polonelli L, Ponton J, Elguezabal N, Moragues MD, Casoli C, Pilotti E, Ronzi P, Dobroff AS, Rodrigues EG, Juliano MA, et al. (2008). Antibody complementarity-determining regions (CDRs) can display differential antimicrobial, antiviral and antitumor activities. *PLoS One* **3**, e2371.

[37] Dobroff AS, Rodrigues EG, Moraes JZ, and Travassos LR (2002). Protective, anti–tumor monoclonal antibody recognizes a conformational epitope similar to melibiose at the surface of invasive murine melanoma cells. *Hybrid Hybridomics* **21**, 321–331.

[38] Bouvet JP, Pires R, and Pillot J (1984). A modified gel filtration technique producing an unusual exclusion volume of IgM: a simple way of preparing monoclonal IgM. *J Immunol Methods* **66**, 299–305.

[39] Paschoalin T, Carmona AK, Oliveira V, Juliano L, and Travassos LR (2005). Characterization of thimet- and neurolysin-like activities in *Escherichia coli* M 3 A peptidases and description of a specific substrate. *Arch Biochem Biophys* **441**, 25–34.

[40] Stone KL and Williams KR (1996). Enzymatic digestion of proteins in solution and in SDS polyacrylamide gels. In *The Protein Protocols Handbook*. JM Walker (Ed). Humana Press, Totowa, NJ. pp. 415–425.

[41] Jurado JD, Rael ED, Lieb CS, Nakayasu E, Hayes WK, Bush SP, and Ross JA (2007). Complement inactivating proteins and intraspecies venom variation in *Crotalus oreganus helleri*. *Toxicon* **49**, 339–350.

[42] Eng JK, McCormack AL, and Yates JR (1994). An approach to correlate tandem mass spectral data of peptides with amino acid sequences in a protein database. *J Am Soc Mass Spectrom* **5**, 976–989.

[43] Nicoletti I, Migliorati G, Pagliacci MC, Grignani F, and Riccardi C (1991). A rapid and simple method for measuring thymocyte apoptosis by propidium iodide staining and flow cytometry. *J Immunol Methods* **139**, 271–279.

[44] Paschoalin T, Carmona AK, Rodrigues EG, Oliveira V, Monteiro HP, Juliano MA, Juliano L, and Travassos LR (2007). Characterization of thimet oligopeptidase and neurolysin activities in B16F10-Nex2 tumor cells and their involvement in angiogenesis and tumor growth. *Mol Cancer* **6**, 44.

[45] Vanhalst K, Kools P, Vanden Eynde E, and van Roy F (2001). The human and murine protocadherin-beta one-exon gene families show high evolutionary conservation, despite the difference in gene number. *FEBS Lett* **495**, 120–125.

[46] Morea V, Tramontano A, Rustici M, Chothia C, and Lesk AM (1998). Conformations of the third hypervariable region in the V_H domain of immunoglobulins. *J Mol Biol* **275**, 269–294.

[47] Levi M, Sallberg M, Ruden U, Herlyn D, Maruyama H, Wigzell H, Marks J, and Wahren B (1993). A complementarity-determining region synthetic peptide acts as a miniantibody and neutralizes human immunodeficiency virus type 1 *in vitro*. *Proc Natl Acad Sci USA* **90**, 4374–4378.

[48] Drebin JA, Link VC, and Greene MI (1988). Monoclonal antibodies specific for the *neu* oncogene product directly mediate anti-tumor effects *in vivo*. *Oncogene* **2**, 387–394.

[49] Trowbridge IS and Domingo DL (1981). Anti-transferrin receptor monoclonal antibody and toxin-antibody conjugates affect growth of human tumour cells. *Nature* **294**, 171–173.

[50] Miyawaki T, Yachie A, Uwadana N, Ohzeki S, Nagaoki T, and Taniguchi N (1982). Functional significance of Tac antigen expressed on activated human T lymphocytes: Tac antigen interacts with T cell growth factor in cellular proliferation. *J Immunol* **129**, 2474–2478.

[51] Masui H, Kawamoto T, Sato JD, Wolf B, Sato G, and Mendelsohn J (1984). Growth inhibition of human tumor cells in athymic mice by anti–epidermal growth factor receptor monoclonal antibodies. *Cancer Res* **44**, 1002–1007.

[52] Oren R, Takahashi S, Doss C, Levy R, and Levy S (1990). TAPA-1, the target of an antiproliferative antibody, defines a new family of transmembrane proteins. *Mol Cell Biol* **10**, 4007–4015.

[53] Hellstrom I, Garrigues HJ, Garrigues U, and Hellstrom KE (1990). Highly tumor-reactive, internalizing, mouse monoclonal antibodies to Le(y)-related cell surface antigens. *Cancer Res* **50**, 2183–2190.

[54] Garrigues J, Garrigues U, Hellstrom I, and Hellstrom KE (1993). Ley specific antibody with potent anti-tumor activity is internalized and degraded in lysosomes. *Am J Pathol* **142**, 607–622.

[55] Frank M and Kemler R (2002). Protocadherins. *Curr Opin Cell Biol* **14**, 557–562.

[56] Wu Q, Zhang T, Cheng JF, Kim Y, Grimwood J, Schmutz J, Dickson M, Noonan JP, Zhang MQ, Myers RM, et al. (2001). Comparative DNA sequence analysis of mouse and human protocadherin gene clusters. *Genome Res* **11**, 389–404.

[57] Zhang T, Haws P, and Wu Q (2004). Multiple variable first exons: a mechanism for cell- and tissue-specific gene regulation. *Genome Res* **14**, 79–89.

[58] Kasemeier-Kulesa JC, Teddy JM, Postovit LM, Seftor EA, Seftor RE, Hendrix MJ, and Kulesa PM (2008). Reprogramming multipotent tumor cells with the embryonic neural crest microenvironment. *Dev Dyn* **237**, 2657–2666.

[59] Oppitz M, Busch C, Schriek G, Metzger M, Just L, and Drews U (2007). Non-malignant migration of B16 mouse melanoma cells in the neural crest and invasive growth in the eye cup of the chick embryo. *Melanoma Res* **17**, 17–30.

[60] Christensen PA, Danielczyk A, Ravn P, Stahn R, Karsten U, and Goletz S (2007). A monoclonal antibody to Lewis Y/Lewis b revealing mimicry of the histone H1 to carbohydrate structures. *Scand J Immunol* **65**, 362–367.

[61] Kato M, Mochizuki K, Kuroda K, Sato S, Murakami H, Yasumoto K, Nomoto K, and Hashizume S (1991). Histone H2B as an antigen recognized by lung cancer–specific human monoclonal antibody HB4C5. *Hum Antibodies Hybridomas* **2**, 94–101.

[62] Raz E, Ben-Bassat H, Davidi T, Shlomai Z, and Eilat D (1993). Cross-reactions of anti-DNA autoantibodies with cell surface proteins. *Eur J Immunol* **23**, 383–390.

[63] Greenberg AH, Chow DA, and Wolosin LB (1983). Natural antibodies: origin, genetics, specificity and role in host resistance to tumours. *Clin Immunol Allergy* **3**, 389–420.

[64] Subiza JL, Coll J, Alvarez R, Valdivieso M, and de la Concha EG (1987). IgM response and resistance to ascites tumor growth. *Cancer Immunol Immunother* **25**, 87–92.

[65] Gil J, Alvarez R, Vinuela JE, Ruiz de Morales JG, Bustos A, De la Concha EG, and Subiza JL (1990). Inhibition of *in vivo* tumor growth by a monoclonal IgM antibody recognizing tumor cell surface carbohydrates. *Cancer Res* **50**, 7301–7306.

[66] Dadachova E, Revskaya E, Sesay MA, Damania H, Boucher R, Sellers RS, Howell RC, Burns L, Thornton GB, Natarajan A, et al. (2008). Pre-clinical evaluation and efficacy studies of a melanin-binding IgM antibody labeled with [188]Re against experimental human metastatic melanoma in nude mice. *Cancer Biol Ther* **7**, 1116–1127.

[67] Revskaya E, Jongco AM, Sellers RS, Howell RC, Koba W, Guimaraes AJ, Nosanchuk JD, Casadevall A, and Dadachova E (2009). Radioimmunotherapy of experimental human metastatic melanoma with melanin-binding antibodies and in combination with dacarbazine. *Clin Cancer Res* **15**, 2373–2379.

[68] Magliani W, Conti S, Maffei DL, Ravanetti L, and Polonelli L (2007). Antiidiotype-derived killer peptides as new potential tools to combat HIV-1 and AIDS-related opportunistic pathogens. *Anti Infective Agents Med Chem* **6**, 263–272.

[69] Magliani W, Conti S, Salati A, Arseni S, Ravanetti L, Frazzi R, and Polonelli L (2004). Engineered killer mimotopes: new synthetic peptides for antimicrobial therapy. *Curr Med Chem* **11**, 1793–1800.

[70] Magliani W, Conti S, Travassos LR, and Polonelli L (2008). From yeast killer toxins to antibiobodies and beyond. *FEMS Microbiol Lett* **288**, 1–8.

[71] Polonelli L, Magliani W, Conti S, Bracci L, Lozzi L, Neri P, Adriani D, De Bernardis F, and Cassone A (2003). Therapeutic activity of an engineered synthetic killer antiidiotypic antibody fragment against experimental mucosal and systemic candidiasis. *Infect Immun* **71**, 6205–6212.

[72] Magliani W, Conti S, Cunha RL, Travassos LR, and Polonelli L (2009). Antibodies as crypts of antiinfective and antitumor peptides. *Curr Med Chem* **16**, 2305–2323.

[73] Litman GW, Cannon JP, and Dishaw LJ (2005). Reconstructing immune phylogeny: new perspectives. *Nat Rev Immunol* **5**, 866–879.

[74] Bourgeois C, Bour JB, Aho LS, and Pothier P (1998). Prophylactic administration of a complementarity-determining region derived from a neutralizing monoclonal antibody is effective against respiratory syncytial virus infection in BALB/c mice. *J Virol* **72**, 807–810.

[75] Xu JL and Davis MM (2000). Diversity in the CDR3 region of V(H) is sufficient for most antibody specificities. *Immunity* **13**, 37–45.

[76] Dorfman T, Moore MJ, Guth AC, Choe H, and Farzan M (2006). A tyrosine-sulfated peptide derived from the heavy-chain CDR3 region of an HIV-1–neutralizing antibody binds gp120 and inhibits HIV-1 infection. *J Biol Chem* **281**, 28529–28535.

[77] Heap CJ, Wang Y, Pinheiro TJ, Reading SA, Jennings KR, and Dimmock NJ (2005). Analysis of a 17–amino acid residue, virus-neutralizing microantibody. *J Gen Virol* **86**, 1791–1800.

[78] Brumatti G, Weinlich R, Chehab CF, Yon M, and Amarante-Mendes GP (2003). Comparison of the anti-apoptotic effects of Bcr-Abl, Bcl-2 and Bcl-X$_L$ following diverse apoptogenic stimuli. *FEBS Lett* **541**, 57–63.